Acid–Base Chemistry of Polypyridyl Ruthenium Compounds of (Pyridin-2′-yl)-1,2,4-triazoles. *X*-Ray Crystal Structure of Bis(2,2′-bipyridine)-[3-methyl-5-(pyridin-2′-yl)-1,2,4-triazolato-*N*¹]ruthenium Hexafluorophosphate Tetrahydrate†

Barbara E. Buchanan and Johannes G. Vos*
School of Chemical Sciences, Dublin City University, Dublin 9, Ireland
Masao Kaneko
Institute of Physical and Chemical Research, Wako-shi, Saitama, 351-01, Japan
Wilhelm J. M. van der Putten and John M. Kelly
Department of Chemistry, Trinity College, University of Dublin, Dublin 2, Ireland
Ronald Hage, Rudolf A. G. de Graaff, Rob Prins, Jaap G. Haasnoot, and Jan Reedijk
Department of Chemistry, Gorlaeus Laboratories, Leiden University, P.O. Box 9502, 2300 RA Leiden, The Netherlands

The acid–base chemistry of the two co-ordination isomers of the complex of bis(2,2′-bipyridyl)-ruthenium(II) $[Ru(bipy)_2]^{2+}$ with 3-(pyridin-2′-yl)-1,2,4-triazole (HL^1) and of the analogous compound with 3-methyl-5-(pyridin-2′-yl)-1,2,4-triazole (HL^2) has been investigated. As expected the ligands act as stronger acids after binding to the $Ru(bipy)_2$ moiety. The two co-ordination isomers of the HL^1 compound show distinctly different pK_a values of 4.07 ± 0.05 and 5.95 ± 0.05. Luminescence titrations and lifetime measurements indicate that both ligands are stronger acids in the excited state than in the ground state. This suggests that they act as spectator ligands and are not directly involved in the photophysical processes. The crystal structure of $[Ru(bipy)_2L^2]PF_6{\cdot}4H_2O$ has been determined by single-crystal *X*-ray diffraction. Crystal data: trigonal, space group $P3_121$ with $a = b = 13.760(6)$, $c = 30.503(9)$ Å, $\alpha = \beta = 90.00$, $\gamma = 120.00°$, and $Z = 6$. The refinement based on 4 288 unique reflections $[I > 2\sigma(I)]$ yielded a $R(R')$ value of 0.036(0.049). The pyridyltriazole ligand is co-ordinated to ruthenium *via* the N^1 atom of the triazolato ring. The Ru–N distances are between 2.050(5) and 2.086(4) Å. Four water molecules have been located near the pyridyltriazole ligand, giving rise to an extended hydrogen-bridged, structure.

In recent publications we reported[1] the synthesis and characterisation of a number of compounds with the general formula $[Ru(bipy)_2(L{-}L')]^{n+}$, where L–L′ is a series of pyridyl-1,2,4-triazole type ligands and bipy = 2,2′-bipyridyl. These compounds are analogues of the extensively studied $[Ru(bipy)_3]^{2+}$, with the important difference that one of the pyridine groups is replaced by a 1,2,4-triazole ring. Also compounds containing pyrazinetriazole and triazinetriazole ligands have recently been prepared.[1d,e] The aim of these studies is to investigate the physical properties of ruthenium compounds containing these ligands. Because of the synthetic versatility available in these ligand systems, the π* levels of the ligands can be finely tuned. As a result the excited-state and electrochemical properties of the ruthenium compounds formed are strongly affected by the nature of the triazole ligand.[1,2]

In the literature much attention has been paid to studies of ruthenium compounds undergoing proton-transfer reactions.[3–12] Such studies are of interest as the acid–base properties of the ground and excited state can often be related to electron-density distributions in the compounds, and it is generally agreed that the excited-state acidity can be related to the nature of the emitting state.[3–7]

In earlier papers[1] the synthesis and chromatographic separation of the two co-ordination isomers of the $Ru(bipy)_2$ complex of 3-(pyridine-2′-yl)-1,2,4-triazole (HL^1), compounds (**1**) and (**2**), of the corresponding complex of 3-methyl-5-(pyridin-2′-yl)-1,2,4-triazole (HL^2), compound (**3**), and of their corresponding triazolato compounds, (**4**)—(**6**) were reported.

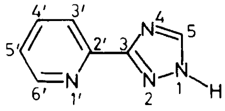

HL^1 (^1H tautomer)

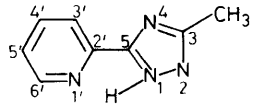

HL^2 (^1H tautomer)

For the HL^2 compound only one isomer was observed. In this contribution we report the acid–base properties of these compounds both in the ground and in the excited state. To ascertain the nature of the co-ordination mode of the HL^2 ligand the *X*-ray structure of the $Ru(bipy)_2$ compound containing the deprotonated ligand, compound (**6**), has been determined.

Results

Description of the Structure of Compound (**6**), $[Ru(bipy)_2L^2]PF_6{\cdot}4H_2O$.—A summary of the crystal data and intensity-collection parameters is given in Table 1 and the fractional co-ordinates are listed in Table 2. A projection of the structure is presented in Figure 1, where for reasons of clarity all P, F, O, and H atoms have been omitted. The relevant bond lengths and angles are listed in Table 3. The ruthenium atom is six-co-

---

† *Supplementary data available:* see Instructions for Authors, *J. Chem. Soc., Dalton Trans.*, 1990, Issue 1, pp. xix—xxii.

ordinated by one pyridyltriazolato and two bipy ligands. The Ru–N distances of between 2.050(5) and 2.086(4) Å are in the normal range for this type of compound, although the latter [Ru–N(51) (pyridine ring of the pyridyltriazolato ligand] is somewhat longer than expected.[13–16] On the other hand the former [Ru–N(1)] distance is shorter than expected for a ruthenium–triazole distance.[17] These differences are possibly explained by the presence of the negative charge on the pyridyltriazolato ligand. The 'bite angles' of all ligands are 78—79°, comparable to chelating angles observed normally for similar structures.[13–17]

As can be seen from Figure 1, the pyridyltriazole ligand is co-ordinated *via* N^1 and $N^{1'}$. This has been predicted from n.m.r. spectroscopy, based on the small shift observed for the methyl resonance upon co-ordination[1a] and is expected for steric reasons because of the presence of the methyl group. Four water molecules have been found near N^4 of the triazole ring. A similar orientation has been observed previously for a similar structure with 3,5-bis(pyridin-2′-yl)-1,2,4-triazole where one oxygen atom was located near the triazole ring.[13] These water molecules give rise to an extensive hydrogen-bonding network; intermolecular O • • • O distances of about 2.8 Å are observed. One oxygen atom [O(1)] is located near N^4 of the triazole ring and linked to O(3); the latter is located near another oxygen atom [O(4)] and finally O(4) is linked with the last water molecule [O(2)], which is in its turn connected to N^2 of the triazole ring of a neighbouring $[Ru(bipy)_2L^2]PF_6$ group. The $[Ru(bipy)_2L^2]^+$ ions in the lattice are all linked by these water molecules. This observation is quite interesting as this might

Table 1. Summary of crystal data and intensity-collection parameters for $[Ru(bipy)_2L^2]PF_6{\cdot}4H_2O$

Formula	$C_{28}H_{31}F_6N_8O_4PRu$
M_r	789.64
Space group	$P3_221$
$a = b$/Å	13.760(6)
c/Å	30.503(9)
U/Å^3	5 003
Z	6
D_m (by flotation)/Mg m^{-3}	1.55
D_c/Mg m^{-3}	1.57
μ(Mo-K_α)/cm^{-1}	5.84
θ Range/°	2—30
Data collection range	*h*, −19 to 19; *k*, 0—19; *l* 0—43
No. of independent reflections	7 867
No. of significant reflections [$I > 2\sigma(I)$]	4 288
F(000)	2 279
R	0.036
R'	0.049
R_{int}	0.010

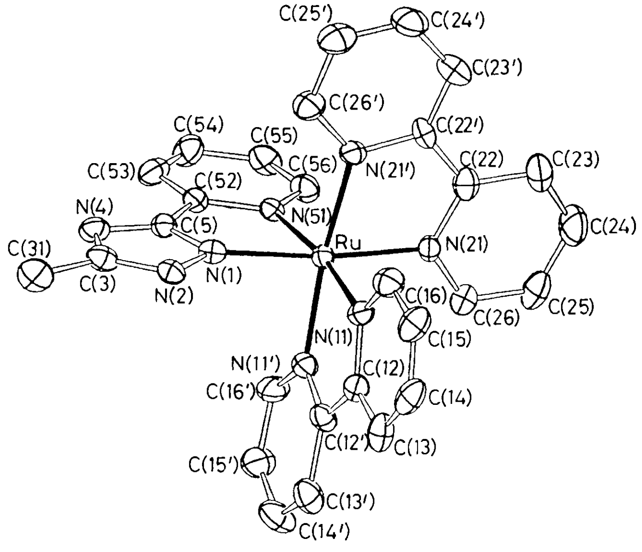

Figure 1. ORTEP drawing of the molecular structure of *cis*-$[Ru(bipy)_2L^2]^+$ (6), showing the atom labelling. Thermal ellipsoids are at 50% probability. The PF_6^- group, the oxygen, and hydrogen atoms have been omitted for clarity

Table 2. Fractional atomic co-ordinates (× 10^5 for Ru; × 10^4 for C, N, F, and O) of $[Ru(bipy)_2L^2]PF_6{\cdot}4H_2O$

Atom	*X*/*a*	*Y*/*b*	*Z*/*c*
Ru	19 465(3)	−14 734(3)	−3 603(1)
P(1)	42 355(20)	42 355(20)	0(0)
F(1)	3 101(4)	3 775(4)	256(2)
F(2)	4 727(5)	5 372(4)	259(2)
F(3)	4 698(4)	3 759(4)	369(2)
P(2)	0(0)	80 590(17)	16 667(0)
F(4)	668(5)	8 396(5)	1 226(1)
F(5)	−805(4)	8 471(3)	1 483(1)
F(6)	−819(4)	6 853(3)	1 490(2)
N(1)	1 093(3)	−2 614(3)	−847(1)
N(2)	1 333(4)	−2 897(4)	−1 248(1)
C(3)	344(5)	−3 647(5)	−1 403(2)
C(31)	179(6)	−4 186(5)	−1 842(2)
N(4)	−535(4)	−3 874(4)	−1 142(2)
C(5)	−31(4)	−3 223(4)	−796(2)
N(51)	298(3)	−2 246(4)	−131(1)
C(52)	−493(4)	−3 044(4)	−394(2)
C(53)	−1 599(5)	−3 600(5)	−287(2)
C(54)	−1 963(5)	−3 386(5)	98(2)
C(55)	−1 193(5)	−2 584(6)	369(2)
C(56)	−49(5)	−2 028(5)	242(2)
N(11)	3 478(3)	−715(4)	−670(1)
C(12)	3 654(4)	128(4)	−949(2)
C(13)	4 667(5)	721(5)	−1 179(2)
C(14)	5 488(5)	422(6)	−1 114(2)
C(15)	5 279(5)	−436(6)	−840(2)
C(16)	4 293(5)	−966(6)	−620(2)
N(11′)	1 815(4)	−313(4)	−734(1)
C(12′)	2 729(5)	339(4)	−993(1)
C(13′)	2 733(6)	1 138(5)	−1 282(2)
C(14′)	1 805(6)	1 271(6)	−1 290(2)
C(15′)	903(6)	621(5)	−1 025(2)
C(16′)	940(5)	−142(5)	−759(2)
N(21)	2 659(3)	−492(3)	187(1)
C(22)	3 031(4)	−954(5)	503(2)
C(23)	3 535(6)	−340(6)	884(2)
C(24)	3 665(7)	686(6)	944(2)
C(25)	3 283(5)	1 150(5)	636(2)
C(26)	2 791(5)	540(4)	256(2)
N(21′)	2 270(3)	−2 516(3)	18(1)
C(22′)	2 849(4)	−2 041(5)	394(2)
C(23′)	3 226(6)	−2 613(6)	651(2)
C(24′)	3 015(6)	−3 685(6)	522(2)
C(25′)	2 414(6)	−4 158(6)	156(2)
C(26′)	2 050(5)	−3 544(5)	−95(2)
O(1)	5 210(4)	7 227(4)	1 394(2)
O(2)	6 851(4)	3 171(4)	1 544(1)
O(3)	6 873(6)	6 611(6)	1 235(2)
O(4)	6 746(6)	4 635(6)	920(2)

Table 3. Selected bond distances (Å) and angles (°) of $[Ru(bipy)_2L^2]PF_6 \cdot 4H_2O$. Data for the bipy rings, the PF_6^- group, and hydrogen atoms have been deposited

Ru-N(1)	2.050(5)	C(3)-N(4)	1.349(8)
Ru-N(51)	2.086(4)	N(4)-C(5)	1.334(7)
Ru-N(11)	2.055(4)	C(5)-C(52)	1.456(8)
Ru-N(11')	2.042(5)	C(52)-N(51)	1.357(7)
Ru-N(21)	2.060(4)	N(51)-C(56)	1.327(7)
Ru-N(21')	2.056(4)	C(56)-C(55)	1.417(9)
N(1)-C(5)	1.349(7)	C(55)-C(54)	1.36(1)
N(1)-N(2)	1.374(6)	C(54)-C(53)	1.367(9)
N(2)-C(3)	1.317(7)	C(53)-C(52)	1.357(9)
C(3)-C(31)	1.493(8)		
N(1)-Ru-N(51)	78.0(2)	N(51)-Ru-N(21')	90.9(2)
N(1)-Ru-N(11)	96.1(2)	N(11)-Ru-N(11')	79.4(2)
N(1)-Ru-N(21')	96.5(5)	N(11)-Ru-N(21)	90.5(2)
N(1)-Ru-N(11')	87.4(2)	N(11')-Ru-N(21)	98.0(2)
N(51)-Ru-N(11')	95.0(2)	N(21)-Ru-N(21')	78.7(2)
N(51)-Ru-N(21)	95.9(2)		

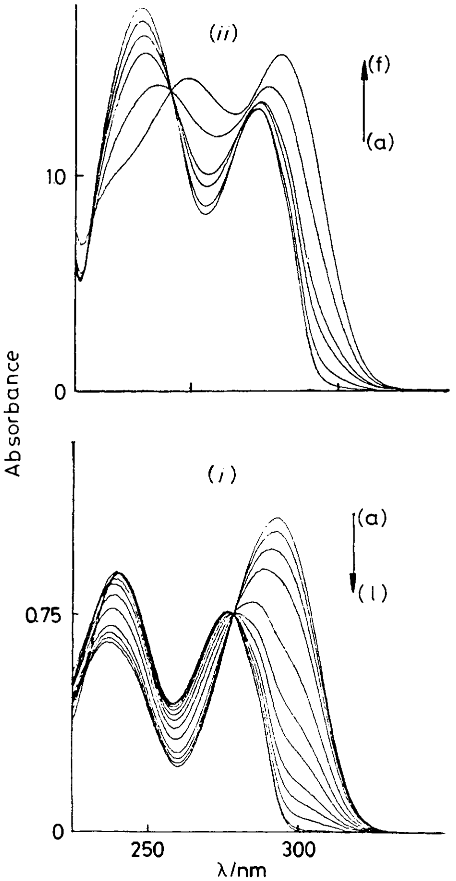

Figure 2. pH Dependence of the absorption spectrum of HL^1 in aqueous Britton–Robinson buffer (1.0 × 10^{-4} mol dm^{-3}). (*i*) For curves (a)—(l): pH 1.21, 2.36, 2.46, 2.89, 3.30, 3.63, 3.84, 4.13, 4.36, 4.69, 5.39, and 6.20. (*ii*) For curves (a)—(f): pH 7.97, 8.89, 9.37, 9.62, 10.16, and 11.00

suggest similar extended hydrogen bonding in 'hydrogen-bonding' solvents, a phenomenon which would effect the photophysical properties of the ruthenium compounds. A similar phenomenon has been observed for $[Ru(bipy)_2Cl_2] \cdot 3.5H_2O$ where water molecules bridge the $[Ru(bipy)_2Cl_2]$ moieties *via* the chlorides.[14]

Table 4. Acid-base properties of the pyridyltriazole ligands: spectroscopic data

Species	Absorption maxima (nm) (log ε)	Emission maximum (nm)
$[H_2L^1]^+$	286 (4.17), 232 (4.24)	435
$[H_2L^2]^+$	290 (4.14), 230 (3.97)	475
HL^1	273 (4.03), 232 (4.12)	370
HL^2	272 (4.06), 235 (4.02)	375
$[L^1]^-$	279 (4.04), 243 (4.11)	435
$[L^2]^-$	283 (4.05), 252 (4.01)	460

Measurements were carried out in Britton–Robinson buffers using 10^{-4} mol dm^{-3} solutions of the ligands for the absorption experiments and 10^{-6} mol dm^3 for the emission studies.

Acid-Base Chemistry of the Free Ligands HL^1 *and* HL^2.—To be able to compare the acid–base chemistry of the co-ordinated ligand with that observed for the free ligands, the pH dependences of their ground-state and excited-state properties were investigated using u.v.–visible and luminescence spectroscopy respectively. All spectral changes observed were reversible. U.v.–visible spectra obtained in a typical experiment with free HL^1 are shown in Figure 2. Both ligands were investigated in the pH range from 1.0 to 11.0. Between pH 1.0 and 6.0 isosbestic points were observed at 272 nm for HL^1 and at 275 nm for HL^2. In this pH range the lowest-energy absorption shifts from about 272 nm at pH 2.0 to 286 nm at pH 6.0. In the pH range from 6.0 to 11.0 isosbestic points were observed at 239 nm for HL^1 and at 243 nm for HL^2 together with shifts to lower energy of both absorption bands with increasing pH (see Table 4).

The pH dependence of the emission of the ligands was investigated over the same pH range. Going from pH 6.0 to 1.0 a significant increase of the emission intensity was observed parallel with a shift of the emission maxima to lower energy (see Table 4). When the data were analysed as emission titrations, inflection points at pH 2.9 ± 0.3 and 3.1 ± 0.3 were found for HL^1 and HL^2, respectively. Going from pH 6.0 to 11.0 again an increase of the emission intensity is observed, combined with an increase in the emission wavelength. In this pH range inflection points were obtained at pH values of 8.9 ± 0.3 and 9.8 ± 0.2 for HL^1 and HL^2, respectively.

Acid–Base Chemistry of Ruthenium Compounds in the Ground State.—H.p.l.c. experiments carried out recently have shown that for the HL^1 compound two isomers are obtained while for the HL^2 complex only one species was isolated. The co-ordination mode of the triazole ring in the two isomers, either N^2 or N^4, was determined by n.m.r. spectroscopy.[1c] Figure 3 shows the effect of a change of pH on the u.v.–visible spectra of the N^4, compound (**1**), and N^2 isomer, compound (**2**). For both isomers isosbestic points at 322, 390, and 458 nm are observed. For the N^4 isomer the $\lambda_{max.}$ of the lowest-energy absorption band shifts from 450 to 470 nm upon decreasing the pH. For the N^2 isomer a shift from 437 to 465 nm is observed under similar conditions. For compound (**3**) a similar behaviour is observed, with isosbestic points at 321, 387, and 456 nm and a shift in the position of the lowest absorption band from 438 to 467 nm on going from low to high pH. All changes are fully reversible and independent of the direction of the pH change. The changes in spectroscopic features for the compounds are summarised in Table 5 and the relevant pK_a(acid) values in Table 6.

Excited-state Properties of the Ruthenium Compounds.—An increase of the pH from 1.0 to 7.0 leads for the N^4 isomer (**1**) to a

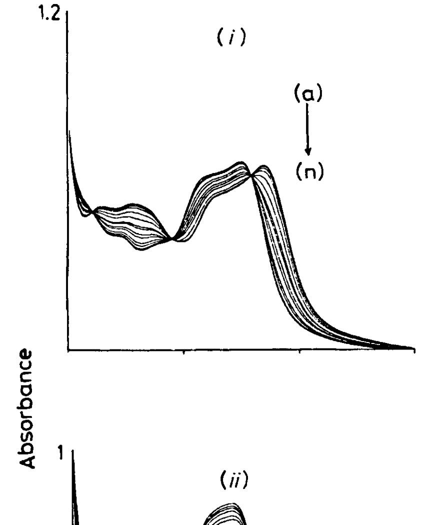

Figure 3. pH Dependence of the absorption spectrum of (*i*) the N^4 and (*ii*) N^2 isomer in an aqueous Britton–Robinson buffer (6.3×10^{-5} mol dm^{-3}). For curves (a)—(n) in (*i*): pH 2.42, 3.52, 4.25, 4.93, 5.16, 5.53, 5.70, 5.95, 6.07, 6.33, 7.07, 7.47, 7.99 and 8.53 and curves (a)—(q) in (*ii*) pH 1.58, 1.93, 2.18, 2.51, 2.97, 3.18, 3.48, 3.70, 3.93, 4.14, 4.35, 4.60, 4.92, 5.33, 5.75, 6.17, and 6.73

Table 5. Excited-state properties of protonated and deprotonated ruthenium compounds

Compound	Absorption maximum (nm)[a] (log ε)	Emission maximum (nm) *a*	*b*	Lifetime[a,c] (ns)	$10^3 \times$ Emission quantum yield[a,d]
(**1**) (N^4)	450 (4.05)	615	580	18 (99), 67 (1)	2.0 ± 0.2
(**2**) (N^2)	437 (4.11)	620	577	30 (90), 15 (10)	1.4 ± 0.2
(**3**)	438 (4.03)	612	587	29 (50), 150 (50)	4.0 ± 0.2
(**4**) (N^4)	470 (3.97)	660	607	145	6.0 ± 0.2
(**5**) (N^2)	465 (4.04)	650	607	110	3.8 ± 0.2
(**6**)	467 (3.93)	645	610	85	2.7 ± 0.2

[a] Data obtained in Britton–Robinson buffer; for compounds (**1**)—(**3**) pH 1.94, for compounds (**4**) and (**5**) pH 8.00. [b] Measured in methanol at 77 K. [c] Values in parentheses are the quantum yields of the different contributions. [d] Values obtained by comparison with $[Ru(bipy)_3]^{2+}$ (quantum yield 0.042).

shift of the emission maximum from 615 to 650 nm, for the other isomer a shift from 620 to 650 is observed, while a shift from 612 to 645 nm is observed for $[Ru(bipy)_2(HL^2)][PF_6]_2$ (**3**) (see Table 5). For both isomers of the HL^1 compound the emission intensity increases with increasing pH. For compound (**3**) on the other hand a decrease of the emission intensity with increasing pH is observed. An example of a typical set of spectra obtained for compound (**1**) is given in Figure 4. The data obtained were analysed as emission titration curves and the inflection points of these curves are given in Table 6. The emission quantum yields and emission lifetimes are given in Table 5. The data in this table show that the emission quantum yields for the compounds reported here are between ten and twenty times lower than those observed for $[Ru(bipy)_3]^{2+}$.[18] The emission lifetime curves were analysed for both single- and double-exponential decays. For all samples, experiments carried out at pH 8.0, the curves could consistently be analysed as single-exponential decays. Experiments carried out at pH 13 gave essentially the same results. However, for the experiments carried out at pH 1.94 the data obtained were best fit as double-exponential decays. Variation of the buffer concentration did not have any effect on the emission intensity.

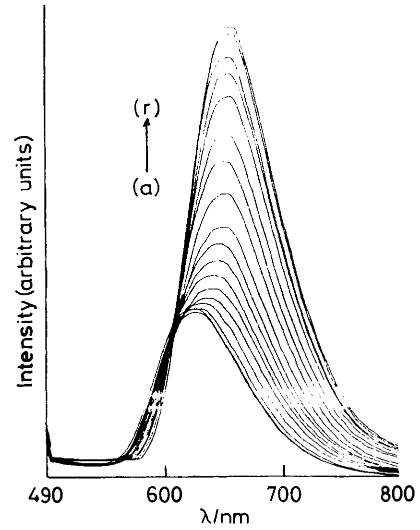

Figure 4. pH Dependence of the emission spectrum of the N^4 isomer in an aqueous Britton–Robinson buffer (1×10^{-5} mol dm^{-3}). For curves (a)—(r): pH 1.64, 2.02, 2.98, 3.66, 4.13, 4.21, 4.31, 4.58, 4.78, 4.92, 5.23, 5.48, 5.72, 5.99, 6.19, 6.46, 6.87, and 7.21

Table 6. Dissociation constants of free and complexed pyridyltriazoles

Compound	pK_a(acid)	pK_a(base)	pK_a^*(acid) *a*	*b*	pK_a^* (base)[b]
HL^1	9.20	3.32	– (8.9)	7.5	6.9 (2.9)
HL^2	9.80	3.40	– (9.8)	6.8	8.3 (3.1)
(**1**) (N^4)	5.95		4.2 (5.1)	4.3	
(**2**) (N^2)	4.07		2.2 (2.8)	2.2	
(**3**)	4.87		4.4 (4.2)	3.5	

Uncertainty in all ground-state pK_a values and inflection points is ± 0.05, excited-state pK_a (pK_a^*) values, ± 0.2; values in parentheses are the inflection points of the emission titration curves.

[a] Calculated using equation (4). [b] Obtained using equation (3), for details see text.

Discussion

The data given above clearly show the pH dependence of the spectroscopic properties of both free ligands and metal complexes. In this section these results are analysed, and the relationship between the acid–base properties of the co-ordinated pyridyltriazole ligands and the electronic properties of the metal complexes is discussed.

Free Ligands.—The spectroscopic changes observed with changing pH can be explained by assuming protonation of the neutral ligands at low pH and deprotonation at higher pH as described in reaction (1). This interpretation is consistent with

$$\mathrm{H_2L^+} \underset{\mathrm{H^+}}{\overset{\mathrm{p}K_a\mathrm{(base)}}{\rightleftharpoons}} \mathrm{HL} \underset{\mathrm{H^+}}{\overset{\mathrm{p}K_a\mathrm{(acid)}}{\rightleftharpoons}} \mathrm{L^-} \qquad (1)$$

experiments carried out with *N*-substituted ligands, such as 4-methyl-3-(pyridin-2′-yl)-4*H*-1,2,4-triazole (L^3). For this ligand a variation of the absorption spectrum was only observed in the pH range from 1 to 6, yielding a pK_a(base) of 4.2 ± 0.2.[19] The pK_a(acid) values observed for the neutral ligands of about 9.50 are somewhat smaller than obtained for 1,2,4-triazole (10.26),[20] while the pK_a(base) values obtained are similar to those reported for pyridine (5.25),[21] 2,2′-bipyridyl (4.45),[22] and 1,2,4-triazole (2.27).[20] From the pK_a(base) values one would expect protonation of the neutral ligand to occur first at the pyridine ring, however hydrogen-bridge formation to the adjacent triazole N atom is likely to influence the location of protonation.

Also the changes in the emission spectra can be rationalised by the occurrence of protonation and deprotonation reactions as described for the ground state. The excited-state properties of the free ligands will be discussed below, together with those observed for the ruthenium compounds.

Ground-state Properties of Ruthenium Compounds.—It is generally agreed that the lowest-energy absorptions, found around 450 nm in the spectra of Ru(bipy)$_2$ compounds, can be described as a singlet metal-to-ligand charge-transfer (^{1}m.l.c.t.) transition, in which the electron is excited from a metal-based *d* orbital to a ligand-based π* orbital. The emission occurs in most of these compounds from a bipy-based ^{3}m.l.c.t. state, which is populated from the singlet state with an efficiency of close to 1.[18,23–25]

The changes in the absorption spectra of the compounds with pH can be explained by deprotonation of the pyridyltriazole ligands at higher pH, yielding respectively [Ru(bipy)$_2$L^1]$^+$ (**4**) and (**5**) and [Ru(bipy)$_2$L^2]$^+$ (**6**) [see equation (2)].

$$\underset{(\mathbf{3})}{[\mathrm{Ru(bipy)_2(HL^2)}]^{2+}} \underset{\mathrm{H^+}}{\overset{\mathrm{p}K_a\mathrm{(acid)}}{\rightleftharpoons}} \underset{(\mathbf{6})}{[\mathrm{Ru(bipy)_2(L^2)}]^{+}} \qquad (2)$$

Results obtained[19] in similar experiments with the compound [Ru(bipy)$_2$L^3]$^{2+}$, where L^3 is the ligand 4-methyl-3-(pyridin-2′-yl)-4*H*-1,2,4-triazole (without possible loss of H$^+$), confirm this interpretation. For this last compound no variation of the absorption spectrum with pH was observed. The changes observed in the absorption spectra of compounds (**1**)—(**3**) upon deprotonation can be explained by an increased electron donation from the deprotonated ligand to the ruthenium(II) centre. This results in a destabilisation of the metal-based ground state and a decrease in the energy of both absorption and emission maxima.[26]

The pK_a values given in Table 6 show that the ligands act as much stronger acids after co-ordination to the Ru(bipy)$_2$ moiety. Similar behaviour has been observed for a number of related ruthenium compounds, such as the Ru(bipy)$_2$ complexes of 4,7-dihydroxy-1,10-phenanthroline, 4,4′-dicarboxy-2,2′-bipyridine,[3,5] 2,2′-benzimidazole,[9,10] and others. The only compound for which an decreased acidity has been observed is [Ru(NH$_3$)$_5$(pyz)]$^{3+}$ (pyz = pyrazine) reported by Ford *et al.*[12] The increased acidity in the compounds reported here can be attributed to electron donation from the pyridyltriazole ligand to the central metal ion. On the other hand the increase in the basicity of the pyrazine ligand on co-ordination has been attributed to strong metal-to-ligand back donation to the pyrazine ligand.[12] So the increased acidity observed for the pyridyltriazole compounds reported here suggests that electron donation from the pyridyltriazole ligands to the Ru^{II} is more important than metal-to-pyridyltriazole back donation. Interestingly, two quite different pK_a values are found for the isomers, with the N^2 species almost two orders of magnitude more acidic than the N^4 compound. This is quite unexpected and suggests that the N^2 atom acts as a much stronger σ donor than the N^4 atom.

When one compares the N^2 isomer with compound (**3**) (in these species the co-ordination mode of the pyridinetriazole ligand is the same) it is clear that the presence of the extra methyl group in HL^2 does not change the ground-state acid–base properties of (**3**) to any great extent. As expected from the electron-donor properties of the methyl group, HL^2 and its Ru(bipy)$_2$ compound are slightly weaker acids.

No evidence was found for further protonation of the co-ordinated ligand to H$_2$L$^+$ at very low pH. This suggests that the basicity of the co-ordinated ligand is strongly reduced. At the same time it should be realised that protonation is hindered by co-ordination of the ligand to the ruthenium ion. Given the fact that pyridine is more basic than 1,2,4-triazole it is worthwhile remembering that protonation of the free ligand occurs most likely at the pyridine nitrogen.

Excited-state Properties.—The changes observed in the emission spectra as a function of pH are consistent with those observed for the absorption spectra and agree with deprotonation of the pyridyltriazole. Surprisingly, deprotonation of HL^1 in the compounds (**1**) and (**2**) leads to a higher emission quantum yield for the resulting compounds (**4**) and (**5**) while for the HL^2 compounds deprotonation of (**3**) leads to a lower emission quantum yield for (**6**).

Using the spectroscopic data obtained for the protonated and deprotonated compounds, an estimate can be made of the excited state pK_a, pK_a*, using the Forster cycle as in equation (3),[26] where T is the absolute temperature, and $\bar{\nu}_a$ and $\bar{\nu}_b$ are the energies (in cm^{-1}) of the (0–0) transition from the ground state to the excited state involved in the deprotonation equilibrium, for the acid and base forms respectively. The results obtained for the free ligands from equation (3), using the lowest-energy

$$\mathrm{p}K_a{}^* = \mathrm{p}K_a + 0.625(\bar{\nu}_b - \bar{\nu}_a)/T \qquad (3)$$

absorption wavelengths as an estimate for the energy of the (0–0) transition, are given in Table 6. If the emission frequencies or the average between emission and absorption maxima are used even more unrealistic results are obtained. The values obtained suggest that, in the excited state, the neutral pyridyltriazole ligands become stronger bases [have a higher pK_a(base)] and stronger acids [have a lower pK_a(acid)]. Similar results were obtained by Aaron and Wineforder[27] in their study of a series of purine derivatives.

An estimate of the pK_a*(acid) values of the ruthenium compounds can be made using the same approach. It seems reasonable to assume that the excited-state acid–base equilibrium will be established in the long-lived triplet state and not in the singlet state that has a much shorter lifetime. So when equation (3) is applied to estimate the pK_a*(acid) of such ruthenium compounds the emission energies should be used, rather than the absorption energies. For our calculations the emission frequencies obtained at 77 K were used, as they are the best means to obtain an estimate for the energy difference involved in the (0–0) transition (see Table 6).

Emission lifetimes of ruthenium compounds. At high pH a single exponential decay of the emission is observed for all species (see Table 5). This strongly suggests the presence of only one emitting state in the species containing a deprotonated pyridyltriazole ligand. On the basis of the electrochemical properties of the compounds [1a] and also because of resonance-Raman data published recently for comparable ruthenium pyridyltriazole compounds,[1d] it is expected that this emitting state is bipy based.

The behaviour observed at low pH is less clear. Best results are obtained using double-exponential fits. From the ground-state pK_a(acid) value it can be calculated that at pH 1.94 less than 1% of compounds (1)—(3) is deprotonated in the ground state. So at this pH only the acid form is excited and the double-exponential decay cannot be caused by a dual excitation. The emission intensities were not affected by the buffer concentration, so quenching by the buffer, as has recently been observed for a series of 1,4,5,8-tetra-azaphenanthrene compounds,[4] can be ruled out.

The nature of the double-exponential decay at low pH is at present not clear, and further investigations, involving temperature-dependent measurements, are needed to clarify the situation. One explanation is that the position of the N–H proton (for example in co-ordinated HL^2 either at N^2 or at N^4) affects the emitting properties of the compounds. In that case the N^4 and N^2 (or N^1) protonated forms are distinctly different species and a double-exponential decay is expected if at least one of the two protonation steps is slow. Alternatively, the presence of two emitting states, one bipy based and one pyridyltriazole based, cannot be ruled out. It is important to note that the lowest-energy absorption maxima observed for the pyridyltriazole ligands are very close to the $\pi \longrightarrow \pi^*$ transition (280 nm) in 2,2′-bipyridyl; this could result in an electronic interaction between these orbitals in the ruthenium compounds. However, on the basis of the earlier mentioned electrochemical and resonance-Raman studies this is not very likely.

The pK_a* values can also be calculated from equation (4),[26]

$$\mathrm{p}K_a{}^* = \mathrm{p}H_i + \log(\tau_a/\tau_b) \qquad (4)$$

where pH_i is the inflection point in the luminescence titration curve and τ_a and τ_b the excited-state lifetimes of the acid and base forms respectively. The pK_a*(acid) values obtained for the ruthenium compounds using equation (4) are listed in Table 6. The presence of a double-exponential decay at high pH makes the application of equation (4) less straightforward. For the two isomers, the most important contribution was used for the calculation. For the HL^2 compound (3) the longest lifetime was used, as for this compound both the emission titration and the quantum yield of emission show an increase in the emission intensity with decreasing pH. In the literature the agreement between the two methods of calculating the excited-state pK_a(acid) values is often not very good, one of the reasons being the difficulty in obtaining the energy for the (0–0) transitions. However, a good agreement is observed in our case.

The pK_a*(acid) values obtained from equations (3) and (4) suggest that the ruthenium compounds are stronger acids in the excited state than in the ground state. This indicates that upon excitation the electron populates a bipy-based π^* orbital. This will create an effective Ru^{III} and result in an increased electron donation from the pyridyltriazole ligands to the central metal atom. A similar increased acidity in the excited state has been observed before for $Ru(bipy)_2$ complexes of 1,2,4-triazole[11] and 4,7-dihydroxy-1,10-phenanthroline.[4]

Conclusion

The *X*-ray structure of compound (6) has substantiated the N^1 co-ordination mode of $(L^2)^-$, in agreement with earlier n.m.r. evidence.[1] The increased acidity of the co-ordinated pyridyltriazole ligands, of about five orders of magnitude, points to electron donation from the ligand to the metal centre, while the increased acidity of the co-ordinated ligand in the excited state suggests that emission occurs from a bipy-based triplet state. A number of unexpected results have been obtained in this study. First, the large difference observed between the pK_a values of the isomers clearly shows the non-equivalence of the triazole N^2 and N^4 co-ordination sites. This difference in electronic properties of the two co-ordination sites has to be taken into account in the investigation of dinuclear systems using pyridyltriazole-type ligands as building blocks.[2] Secondly, the fact that the emission intensity for both isomers of the HL^1 compounds increases with pH, while for (3) under the same conditions a decrease is observed, is quite surprising. Finally, the double-exponential decay observed for the emission lifetime curves is at present not understood. More detailed investigations including temperature-dependence measurements and also an investigation of solvent interactions will be needed to elucidate these features.

Experimental

The compounds $[Ru(bipy)_2(HL^1)][PF_6]_2$ (1) and (2) and $[Ru(bipy)_2(HL^2)][PF_6]_2$ (3) were obtained as described before.[1] The chromatographic separation of the co-ordination isomers (1) and (2) is reported elsewhere.[1b,c] To facilitate dissolution in aqueous solutions the compounds were obtained as the dichloride salts by addition of some dilute HCl and subsequent precipitation in acetone, or by using Amberlite IRA-400 (Cl) as an ion-exchange resin. Solutions were buffered in the range pH 1.9—13, using a Britton–Robinson buffer (0.04 mol dm^{-3} acetic acid, 0.04 mol dm^{-3} phosphoric acid, and 0.04 mol dm^{-3} boric acid); the pH of the buffer solutions was adjusted using 1.0 mol dm^{-3} NaOH solutions.

Instrumental Procedures.—U.v.–visible spectra were obtained using a Shimadzu UV 240 instrument. Emission spectra were obtained on a Perkin-Elmer LS-5 luminescence spectrometer equipped with a red-sensitive Hamamatsu R 928 photomultiplier tube. As the shifts in emission spectra between the different compounds are relatively small, the data obtained were not corrected for photomultiplier response. Luminescence titrations were carried out using an appropriate isosbestic point as the excitation wavelength. So the excitation wavelength for the free ligands was 270 nm for the range pH 1—6, 240 nm for the range pH 6—10, and 455 nm for the ruthenium compounds. Emission quantum yields were measured with respect to $[Ru(bipy)_3]^{2+}$,[18] using a Spectrophysics SP4270 integrator. Lifetime measurements were carried out using time-correlated single-photon counting. Two different instruments were used. Apart from the excitation wavelength the experimental conditions used were the same. For experiments using an excitation wavelength of 438 nm a Hitachi-Horiba NAES-1100 instrument was used. An Applied Photophysics apparatus was used for measurements carried out with an excitation wavelength of 337 nm. This instrument consists of a nitrogen-filled lamp (pulse width *ca.* 3 ns), a Philips XP2233B stop photomultiplier, ORTEC EEG 474, 473A, and 457 signal-processing modules, and a Canberra series 30 multichannel analyser.

All samples were degassed with argon for 10 min. The accuracy of the system was checked by using standard solutions of quinine sulphate and $[Ru(bipy)_3]^{2+}$.[18,28]

X-Ray Data Collection.—A red octahedrally shaped crystal (dimensions 0.5 × 0.3 × 0.3 mm) of bis(2,2′-bipyridine)[3-methyl-5-(pyridine-2′-yl)-1,2,4-triazolato-*N*^{1}]ruthenium hexafluorophosphate tetrahydrate, $[Ru(bipy)_2L^2]PF_6 \cdot 4H_2O$ was selected to determine the molecular structure. The diffraction data were collected at room temperature on an Enraf-Nonius CAD-4 automatic four-circle diffractometer with graphite-monochromated Mo-K_α radiation ($\lambda = 0.710\,73$ Å). To measure any deterioration of the crystal, the intensity data were checked periodically (every 90 min), by using selected intensity standards. The data were corrected for Lorentz and polarisation effects. No correction for absorption was applied. Atomic scattering factors for neutral atoms were taken from the literature.[29] Details of crystal data and intensity collection are given in Table 1.

Solution and refinement of the structure. The structure was solved in space group $P3_121$. The position of the ruthenium atom was obtained using standard Patterson techniques and the program AUTOFOUR.[30] The positions of the P, F, O, N, and C atoms were found using Fourier synthesis and successive cycles of least-squares refinement, based on 4 288 unique reflections [with $I > 2\sigma(I)$]. The function minimised was $[w(|F_o| - |F_c|)^2]$ with $w = 1/\sigma_F{}^2$. All non-hydrogen atoms were given individual anisotropic thermal parameters in the refinement. A Fourier difference map yielded the positions of all hydrogen atoms, except for those of two water molecules. The phosphorus atoms are located at special positions, $[(x,x,0)$ and $(0,x,\frac{1}{6})]$ on a two-fold axis. Reliability indices referred to in Table 1 are $R = \Sigma||F_o| - |F_c||/\Sigma|F_o|$ and $R' = [\Sigma w(|F_o| - |F_c|)^2/\Sigma w|F_o|^2]^{\frac{1}{2}}$. The positional parameters of all non-hydrogen atoms are listed in Table 2.

Additional material available from the Cambridge Crystallographic Data Centre comprises H-atom co-ordinates, thermal parameters, and remaining bond lengths and angles.

Acknowledgements

The authors thank EOLAS, the Irish Science and Technology Agency, for financial assistance, J. G. V. thanks the Riken Institute for a generous travel grant. Ing. S. Gorter is thanked for collecting the *X*-ray data.

References

1 (*a*) R. Hage, R. Prins, J. G. Haasnoot, J. Reedijk, and J. G. Vos, *J. Chem. Soc., Dalton Trans.*, 1987, 1389; (*b*) B. E. Buchanan, E. McGovern, P. Harkin, and J. G. Vos, *Inorg. Chim. Acta*, 1988, **154**, 1; (*c*) B. E. Buchanan, R. Wang, J. G. Vos, R. Hage, J. G. Haasnoot, and J. Reedijk, *Inorg. Chem.*, in the press; (*d*) R. Hage, J. G. Haasnoot, D. J. Stufkens, T. L. Snoeck, J. G. Vos, and J. Reedijk, *Inorg. Chem.*, 1989, **28**, 1413; (*e*) R. Hage, J. H. van Diemen, G. Ehrlich, J. G. Haasnoot, D. J. Stufkens, T. L. Snoeck, J. G. Vos, and J. Reedijk, *ibid.*, 1990, **29**, 988.

2 R. Hage, A. H. J. Dijkhuis, J. G. Haasnoot, R. Prins, J. Reedijk, B. E. Buchanan, and J. G. Vos, *Inorg. Chem.*, 1988, **27**, 2185.

3 P. J. Giordano, C. R. Bock, M. S. Wrighton, L. V. Interrante, and R. F. X. Williams, *J. Am. Chem. Soc.*, 1977, **99**, 3187; P. J. Giordano, C. R. Bock, and M. S. Wrighton, *ibid.*, 1978, **100**, 6960.

4 A. Kirsch-De Mesmaeker, L. Jaquet, and J. Nasielsky, *Inorg. Chem.*, 1988, **27**, 4451.

5 T. Shimidzu, T. Iyoda, and K. Izaki, *J. Phys. Chem.*, 1985, **89**, 642.

6 R. J. Crutchley, N. Kress, and A. B. P. Lever, *J. Am. Chem. Soc.*, 1983, **105**, 1170.

7 S. H. Peterson and J. N. Demas, *J. Am. Chem. Soc.*, 1979, **101**, 6571.

8 A. Juris, F. Barigelletti, V. Balzani, P. Belser, and A. von Zelewsky, *J. Chem. Soc., Faraday Trans. 2*, 1987, **83**, 2295.

9 M. Haga, *Inorg. Chim. Acta*, 1983, **75**, 29.

10 A. M. Bond and M. Haga, *Inorg. Chem.*, 1986, **25**, 4507.

11 C. Long and J. G. Vos, *Inorg. Chim. Acta*, 1984, **89**, 125.

12 P. Ford, D. F. P. Rudd, R. Gaunder, and H. Taube, *J. Am. Chem. Soc.*, 1968, **90**, 1187.

13 R. Hage, J. P. Turkenburg, R. A. G. de Graaff, J. G. Haasnoot, J. Reedijk, and J. G. Vos, *Acta Crystallogr., Sect. C*, 1989, **45**, 381.

14 D. S. Eggleston, K. A. Goldsby, D. J. Hodgson, and T. J. Meyer, *Inorg. Chem.*, 1985, **24**, 4573.

15 D. P. Rillema, D. S. Jones, and H. Levy, *J. Chem. Soc., Chem. Commun.*, 1979, 849.

16 R. P. Thummel, F. Lefoulon, and J. D. Korp, *Inorg. Chem.*, 1987, **26**, 2370.

17 R. Hage, R. Prins, R. A. G. de Graaff, J. G. Haasnoot, J. Reedijk, and J. G. Vos, *Acta Crystallogr., Sect. C*, 1988, **44**, 56; Z. Hu, Y. Lin, S. Jin, and J. G. Vos, *ibid.*, 1989, **45**, 1490.

18 J. van Houten and R. J. Watts, *J. Am. Chem. Soc.*, 1976, **98**, 4853.

19 B. E. Buchanan, unpublished work.

20 K. T. Potts, in 'Comprehensive Heterocyclic Chemistry,' vol. 5, eds. A. R. Katritzky and C. W. Rees, Pergamon, Oxford, 1984.

21 A. J. Boulton and A. McKillop, in 'Comprehensive Heterocyclic Chemistry,' vol. 5, eds. A. R. Katritzky and C. W. Rees, Pergamon, Oxford, 1984.

22 K. Nakamoto, *J. Phys. Chem.*, 1960, **64**, 1420.

23 E. M. Kober and T. J. Meyer, *Inorg. Chem.*, 1984, **23**, 3877.

24 E. A. Seddon and K. R. Seddon, 'The Chemistry of Ruthenium,' Elsevier, Amsterdam, 1984.

25 B. P. Sullivan, D. J. Salmon, and T. J. Meyer, *Inorg. Chem.*, 1979, **18**, 3369.

26 J. F. Ireland and P. A. H Wyatt, *Adv. Phys. Org. Chem.*, 1976, **12**, 131.

27 J. J. Aaron and J. D. Wineforder, *Photochem. Photobiol.*, 1973, **18**, 97.

28 R. A. Lampert, L. A. Chewter, D. Phillips, D. V. O'Conner, A. J. Roberts, and S. R. Meech, *Anal. Chem.*, 1983, **55**, 68.

29 'International Tables for *X*-Ray Crystallography,' Kynoch Press, Birmingham, 1974, vol. 19.

30 A. J. Kinneging and R. A. G. de Graaff, *J. Appl. Crystallogr.*, 1984, **17**, 364.

Received 22*nd January* 1990; *Paper* 0/00345J